

# Synthesis and Charge-Carrier Transport Properties of Poly(phosphole *P*-alkanesulfonylimide)s

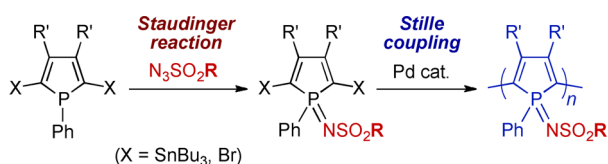
Yoshihiro Matano,<sup>\*,†</sup> Hiroshi Ohkubo,<sup>†</sup> Yoshihito Honsho,<sup>‡</sup> Arihiro Saito,<sup>†</sup> Shu Seki,<sup>\*,‡</sup> and Hiroshi Imahori<sup>§</sup>

Department of Molecular Engineering, Graduate School of Engineering, Kyoto University, Nishikyo-ku, Kyoto 615-8510, Japan, Department of Applied Chemistry, Graduate School of Engineering, Osaka University, Suita, Osaka 565-0871, Japan, and Institute for Integrated Cell-Material Sciences (WPI-iCeMS), Kyoto University, Nishikyo-ku, Kyoto 615-8510, Japan

matano@scl.kyoto-u.ac.jp; seki@chem.eng.osaka-u.ac.jp

Received January 12, 2013

## ABSTRACT



A new class of polyphospholes bearing alkanesulfonylimino moieties on the phosphorus(V) centers was prepared by the Pd–CuI-promoted Stille coupling reaction to investigate the charge-carrier transport properties of the  $\pi$ -networks of polyphospholes. Time-of-flight measurements have revealed that the poly(phosphole *P*-imide)s possess ambipolar charge-carrier mobilities of up to  $\mu_{\text{electron}} = 6 \times 10^{-3} \text{ cm}^2 \text{ V}^{-1} \text{ s}^{-1}$  and  $\mu_{\text{hole}} = 4 \times 10^{-3} \text{ cm}^2 \text{ V}^{-1} \text{ s}^{-1}$ .

Conjugated polymers consisting of heterocyclopentadienes are one of the most intensively studied polymer materials because of their intriguing optical and semiconducting properties derived from the heteroatom-bridged polyacetylene  $\pi$ -networks. In particular, polythiophene derivatives such as poly(3-hexylthiophene) (P3HT) have been frequently used as p-type semiconductors in organic electronics.<sup>1</sup> Considering the large demand for further

extension of the wet-process fabrication of organic electronics, it is also necessary to explore polymer-based n-type semiconductors in terms of materials supply. For example, a naphthalenediimide–bithiophene-based conjugated polymer, P(NDI2OD-T2),<sup>2</sup> has recently emerged as a viable candidate for high-mobility organic electron-transport material.<sup>3</sup> To our knowledge, however, little attention has been paid to heterole-based conjugated polymers with high electron mobility.

Among several approaches to improve the electron affinity of conjugated  $\pi$ -systems, incorporation of phosphacyclopentadiene (phosphole) is highly promising.<sup>4</sup> This is partly because phosphole has an intrinsically low-lying LUMO as a result of the effective  $\sigma_{\text{P}-\text{X}}^* - \pi_{\text{C}=\text{C}}^*$  orbital

<sup>†</sup> Department of Molecular Engineering, Kyoto University.

<sup>‡</sup> Osaka University.

<sup>§</sup> WPI-iCeMS, Kyoto University.

(1) For example, see: (a) *Handbook of Thiophene-Based Materials; Applications in Organic Electronics and Photonics*; Perepichka, I. F., Perepichka, D. F., Eds.; John Wiley & Sons: West Sussex, DC, 2009. (b) Heeger, A. J.; Sariciftci, N. S.; Nanddas, E. B. *Semiconducting and Metallic Polymers*; Oxford University Press: New York, 2010. (c) Kim, F. S.; Ren, G.; Jenekhe, S. A. *Chem. Mater.* **2011**, *23*, 682 and references cited therein.

(2) P(NDI2OD-T2): Poly[*N,N*-bis(2-octyldodecyl)naphthalene-1,4,5,8-bis(dicarboximide)-2,6-diyl-alt-5,5'-2,2'-bithiophene]. (a) Yan, H.; Chen, Z.; Zheng, Y.; Newman, C.; Quinn, J. R.; Dötz, F.; Kastler, M.; Facchetti, A. *Nature* **2009**, *457*, 679. (b) Caironi, M.; Newman, C.; Moore, J. R.; Natali, D.; Yan, H.; Facchetti, A.; Sirringhaus, H. *Appl. Phys. Lett.* **2010**, *96*, 183303. (c) Steyrleuthner, R.; Schubert, M.; Jaiser, F.; Blakesley, J. C.; Chen, Z.; Facchetti, A.; Neher, D. *Adv. Mater.* **2010**, *22*, 2799. (d) Steyrleuthner, R.; Schubert, M.; Howard, I.; Klaumünzer, B.; Schilling, K.; Chen, Z.; Saalfrank, P.; Laquai, F.; Facchetti, A.; Neher, D. *J. Am. Chem. Soc.* **2012**, *134*, 18303 and references cited therein.

(3) Blakesley, J. C.; Schubert, M.; Steyrleuthner, R.; Chen, Z.; Facchetti, A.; Neher, D. *Appl. Phys. Lett.* **2011**, *99*, 183310.

(4) For example, see: (a) Mathey, F. *Angew. Chem., Int. Ed.* **2003**, *42*, 1578. (b) Hissler, M.; Dyer, P. W.; Réau, R. *Coord. Chem. Rev.* **2003**, *244*, 1. (c) Quin, L. D. *Curr. Org. Chem.* **2006**, *10*, 43. (d) Baumgartner, T.; Réau, R. *Chem. Rev.* **2006**, *106*, 4681. Correction: **2007**, *107*, 303. (e) Réau, R.; Dyer, P. W. In *Comprehensive Heterocyclic Chemistry III*; Ramsden, C. A., Scriven, E. F. V., Taylor, R. J. K., Eds.; Elsevier: Oxford, 2008; Chapter 3.15, pp 1029–1048. (f) Matano, Y.; Imahori, H. *Org. Biomol. Chem.* **2009**, *7*, 1258. (g) Ren, Y.; Baumgartner, T. *Dalton Trans.* **2012**, *41*, 7792.

interaction. More importantly, the electron-accepting ability of the phosphole-based  $\pi$ -systems can be largely enhanced by the oxidation of the phosphorus center from  $P^{III}$  to  $P^V$ . Indeed, precisely designed arene-fused phosphole  $P$ -oxides and  $P$ -sulfides have evolved as a new class of low-molecular-weight n-type semiconductors.<sup>5,6</sup> The solubility and polarity of phosphole-based  $\pi$ -systems can also be tuned by the substituents at  $P$ -sites.

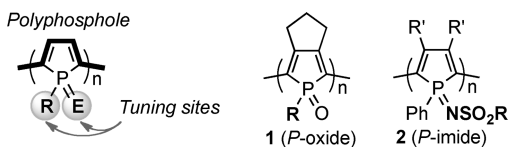
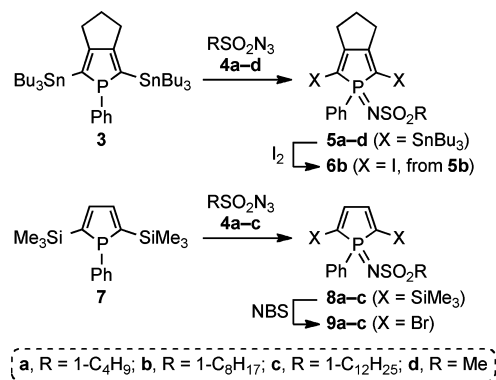


**Figure 1.** Tuning sites of  $\sigma^4$ -P polyphospholes **1** and **2**.

The electronic features of phosphole could be useful in the  $\pi$ -networks of conjugated polymers (Figure 1), and there have been some theoretical studies on unsubstituted polyphosphole.<sup>7</sup> However, the experimental research on polyphosphole derivatives has been left untouched until recently.<sup>8</sup> In 2010, we reported the first example of poly(phosphole  $P$ -oxide) (**1**,  $R = p\text{-C}_{12}\text{H}_{25}\text{OC}_6\text{H}_4$ ; Figure 1), which has been proven to possess a high electron affinity and a narrow HOMO–LUMO gap compared with P3HT.<sup>9</sup> These findings motivated us to develop polyphospholes bearing  $\sigma^4$ -phosphorus(V) centers as a new class of polymer-based n-type semiconductors. We report herein the first synthesis and charge-carrier transport properties of poly(phosphole  $P$ -alkanesulfonylimides) **2** (Figure 1).

Scheme 1 depicts the syntheses of phosphole monomers bearing iminophosphoryl ( $\sigma^4\text{-P}^V=\text{N}$ ) moieties, which include the Staudinger reaction as a key step for the introduction of solubilizing alkyl chains onto the phosphorus centers. One of the advantages of this protocol is that a series of monomers with different alkyl chains are available from the common phosphole synthons. 2,5-Bis(tributylstannyl)phosphole **3**, generated *in situ* from 1,7-bis(tributylstannyl)hepta-1,6-diyne according to the reported procedure,<sup>9</sup> reacted with four kinds of alkane-1-sulfonyl azides **4a–d** to

**Scheme 1.** Synthesis of Phosphole Monomers **5a–d**, **6b**, and **9a–c**.



give the corresponding 2,5-bis(tributylstannyl)phosphole  $P$ -sulfonimides **5a–d** accompanied by the evolution of nitrogen gas. Iodolysis of the C–Sn bonds of **5b** with  $\text{I}_2$  afforded 2,5-diiodophosphole  $P$ -imide **6b**. To obtain the polyphosphole, we conducted a Stille coupling reaction between **5b** and **6b** in the presence of a palladium catalyst and  $\text{CuI}$ ;<sup>9</sup> however, the expected polymerization did not proceed smoothly even after prolonged heating. This may be partly attributable to the steric congestion induced by the  $P$ - and  $\beta$ -substituents on the phosphole ring. We therefore decided to use  $\beta$ -unsubstituted phospholes as a part of monomers. Reaction of 2,5-bis(trimethylsilyl)phosphole **7**<sup>10</sup> with **4a–c** afforded  $\beta$ -unsubstituted phosphole  $P$ -sulfonimides **8a–c**, which were subsequently transformed to 2,5-dibromophospholes **9a–c** by treatment with  $N$ -bromosuccinimide (NBS).

As expected, Stille coupling between **5b** and **9b** under the Pd–CuI catalysis conditions proceeded smoothly at rt to give the target poly(phosphole  $P$ -octylsulfonimide) **2b** within a few hours (Scheme 2). The polymer **2b** was isolated as a deep blue solid by repeated precipitations from  $\text{CH}_2\text{Cl}_2$ –MeOH and  $\text{CH}_2\text{Cl}_2$ –hexane. The number-average molecular weight ( $M_n$ ) and polydispersity index (PDI) of **2b** were determined by gel permeation chromatography as 24 000 and 1.8, respectively, relative to polystyrene standards (Figure S1 in the Supporting Information, SI). With the same catalysis system, poly(phosphole  $P$ -imide)s **2a** ( $M_n = 24\,000$ , PDI = 1.6) and **2c** ( $M_n = 24\,000$ , PDI = 1.9) were prepared from the corresponding monomers **5a/9a** and **5c/9c** (Scheme 2). The polymers **2a–c** showed two branches of broad  $^{31}\text{P}$  NMR peaks at  $\delta_{\text{P}}$  2–6 and 23–28 ppm in  $\text{CD}_2\text{Cl}_2$ , which were assignable to the  $^{31}\text{P}$  nuclei of  $\beta$ -unsubstituted and  $\beta$ -substituted phosphole units, respectively. In the IR spectra, **2a–c** displayed P=N stretching vibration bands at  $\nu_{\text{max}}$  1261–1266  $\text{cm}^{-1}$ .

The  $P$ -imide monomer **10** (Figure 2) was prepared by Stille coupling of **5a** with iodobenzene, and its structure

(5) (a) Tsuji, H.; Sato, K.; Ilies, L.; Itoh, Y.; Sato, Y.; Nakamura, E. *Org. Lett.* **2008**, *10*, 2263. (b) Tsuji, H.; Sato, K.; Sato, Y.; Nakamura, E. *J. Mater. Chem.* **2009**, *19*, 3364. (c) Tsuji, H.; Sato, K.; Sato, Y.; Nakamura, E. *Chem.—Asian J.* **2010**, *5*, 1294.

(6) (a) Matano, Y.; Miyajima, T.; Fukushima, T.; Kaji, H.; Kimura, Y.; Imahori, H. *Chem.—Eur. J.* **2008**, *14*, 8102. (b) Saito, A.; Miyajima, T.; Nakashima, M.; Fukushima, T.; Kaji, H.; Matano, Y.; Imahori, H. *Chem.—Eur. J.* **2009**, *15*, 10000. (c) Matano, Y.; Saito, A.; Fukushima, T.; Tokudome, Y.; Suzuki, F.; Sakamaki, D.; Kaji, H.; Ito, A.; Tanaka, K.; Imahori, H. *Angew. Chem., Int. Ed.* **2011**, *50*, 8016. (d) Matano, Y.; Saito, A.; Suzuki, Y.; Miyajima, T.; Akiyama, S.; Otsubo, S.; Nakamoto, E.; Aramaki, S.; Imahori, H. *Chem.—Asian J.* **2012**, *7*, 2305.

(7) (a) Salzner, U.; Lagowski, J. B.; Pickup, P. G.; Poirier, R. A. *Synth. Met.* **1998**, *96*, 177. (b) Ma, J.; Li, S.; Jiang, Y. *Macromolecules* **2002**, *35*, 1109. (c) Casanovas, J.; Alemán, C. *J. Phys. Chem. C* **2007**, *111*, 4823. (d) Zhang, G.; Ma, J.; Wen, J. *J. Phys. Chem. B* **2007**, *111*, 11670.

(8) Chain-type  $\alpha,\alpha'$ -conjugated quaterphospholes and terphospholes: (a) Deschamps, E.; Ricard, L.; Mathey, F. *Angew. Chem., Int. Ed. Engl.* **1994**, *33*, 1158. (b) Matano, Y.; Nakashima, M.; Imahori, H. *Angew. Chem., Int. Ed.* **2009**, *48*, 4002.

(9) Saito, A.; Matano, Y.; Imahori, H. *Org. Lett.* **2010**, *12*, 2675.

(10) Nief, F.; de Borms, T. B.; Ricard, L.; Carmichael, D. *Eur. J. Inorg. Chem.* **2005**, 637.

(11)  $\text{C}_{26}\text{H}_{24}\text{NO}_2\text{PS}$ , MW = 445.49,  $0.40 \times 0.15 \times 0.10 \text{ mm}^3$ , orthorhombic,  $Pbca$ ,  $a = 11.060(3) \text{ \AA}$ ,  $b = 18.268(5) \text{ \AA}$ ,  $c = 21.576(6) \text{ \AA}$ ,  $V = 4359.1(19) \text{ \AA}^3$ ,  $Z = 8$ ,  $\rho_{\text{calcd}} = 1.358 \text{ g cm}^{-3}$ ,  $\mu = 2.46 \text{ cm}^{-1}$ , collected 30 161, independent 4912, parameters 280,  $R_w = 0.1424$ ,  $R = 0.0568$  ( $I > 2.0\sigma(I)$ ), GOF = 1.044.

**Scheme 2.** Synthesis of Poly(phosphole *P*-imide)s **2a–c**.

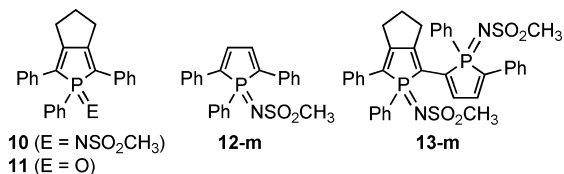
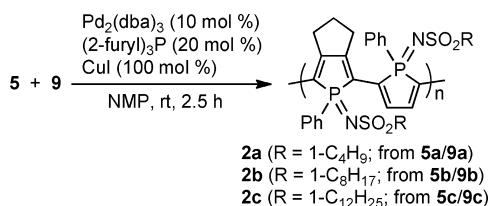


**Figure 2.** Phosphole monomers and dimers.

was elucidated by X-ray analysis.<sup>11</sup> As shown in Figure S2, the P-center in **10** adopts a distorted tetrahedral geometry and is weakly coordinated by one of the sulfonyl O-atoms, O1. Due to the intramolecular O1-to-P coordination, the methyl group on the S-atom is oriented diagonally against the P–N bond with the P–N–S–C torsion angle of 115.4(2)°.

Figure 3 shows the UV/vis absorption spectra of the polymers (**1** and **2a–c**) and the monomers (**10** and **11**) in CH<sub>2</sub>Cl<sub>2</sub>. The red-shifted absorptions upon substituting P=O (**1**,  $M_n = 13\,000$ , PDI = 2.3;  $\lambda_{\text{max}} = 655$  nm) for P=NSO<sub>2</sub>R (**2a–c**;  $\lambda_{\text{max}} = 674\text{--}684$  nm) imply that the P=NSO<sub>2</sub>R bridges relative to the P=O bridge narrow the band gap of the  $\pi$ -network of polyacetylene more effectively. Indeed, both absorption and emission maxima of the *P*-imide monomer **10** ( $\lambda_{\text{abs}} = 395$  nm,  $\lambda_{\text{em}} = 510$  nm) are red-shifted relative to those of the *P*-oxide monomer **11** (Figure 2;  $\lambda_{\text{abs}} = 386$  nm,  $\lambda_{\text{em}} = 491$  nm).<sup>9</sup> It is worth noting that **2a–c** can absorb a wide range of vis/NIR light reaching 1000 nm. In this regard, poly(phosphole *P*-imide)s fulfill a prerequisite for low band gap polymer materials. The reduction potential ( $E_{\text{red}}$ ) of **10** (–1.85 V vs ferrocene/ferrocenium, determined by cyclic voltammetry in CH<sub>2</sub>Cl<sub>2</sub> with Bu<sub>4</sub>NPF<sub>6</sub>; Figure S3) is shifted to the positive side compared with the  $E_{\text{red}}$  value of **11** (–2.02 V), indicating that the P=NSO<sub>2</sub>R group enhances the electron-accepting ability of the P-bridged  $\pi$ -system more significantly than the P=O group. In our hands, redox potentials of **2a–c** could not be determined accurately by cyclic voltammetry probably due to the low effective concentration of the polymer on the electrode surface.

To complement the electronic structures and geometries of **1** and **2**, density functional theory (DFT) calculations on monomers (**10** and **11**) and monomer/dimer models (Figure 2; **12-m** and **13-m**) were performed at the B3LYP/6-31G\* level (Figures S4 and S5). In each compound, the HOMO is spread over the entire  $\pi$ -system,

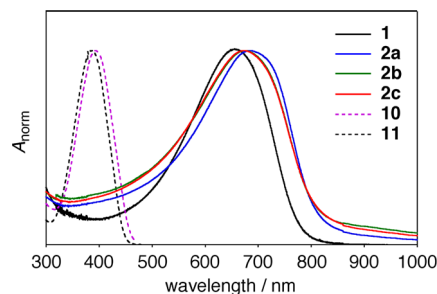


**Figure 3.** UV/vis absorption spectra of **1**, **2**, **10**, and **11** in CH<sub>2</sub>Cl<sub>2</sub>.

whereas the LUMO displays typical  $\sigma^*-\pi^*$  interaction in the phosphole rings. The LUMO level of **10** (–2.16 eV) is lower than that of **11** (–1.93 eV), which is in good accordance with the observed  $E_{\text{red}}$  values. The dimerization from **10/12-m** to **13-m** lowers the LUMO level, raises the HOMO level, and, as a result, significantly narrows the HOMO–LUMO gap of the  $\pi$ -system from 3.43/3.41 to 2.64 eV. The two phosphole rings in *anti*-**13-m** are coplanar with the P–C–C–P torsion angle of 180°, which suggests that the  $\pi$ -network is highly conjugated through the inter-ring C–C bond.

To evaluate the charge transport abilities of poly-(phosphole *P*-imide)s, we measured the electron mobility ( $\mu_e$ ) and hole mobility ( $\mu_h$ ) of thin films of **2a,b** at rt using a time-of-flight (TOF) method (for details, see SI). As shown in Figure 4a,b, the TOF current transients observed at the positive and negative biases showed similar decay profiles, indicating that **2a,b** possess ambipolar charge-transport character. As shown in Figure 4c,d, the charge carrier mobilities displayed negative dependence on the electric field strength ( $E$ ). It seems that the carrier trapping occurs with a larger probability as the applied voltage increases. This is reasonable, considering that **2a,b** exhibit intra- and interchain hopping events of their polymer  $\pi$ -networks. Table 1 summarizes the  $\mu_e$  and  $\mu_h$  values observed at  $E = 1.8 \times 10^4$  V cm<sup>–1</sup> as well as those at  $E = 0$ , obtained by extrapolation of plots of the logarithm values of  $\mu_e$  and  $\mu_h$  as a function of  $E^{1/2}$ . The alkyl chains on the sulfonimide moieties affect the charge-carrier transport properties; the  $\mu_e$  and  $\mu_h$  values of the octyl derivative **2b** are larger than the respective values of the butyl derivative **2a**. This might reflect the difference in the intermolecular segregation of the polymer chains between **2a** and **2b**. The TOF electron mobilities of **2a,b** are lower than that of P(NDI2OD-T2) ( $6 \times 10^{-2}$  cm<sup>2</sup> V<sup>–1</sup> s<sup>–1</sup>).<sup>3</sup> It should be noted, however, the present poly(phosphole *P*-imide)s transport not only electrons but also holes with almost the same efficiency ( $\mu_e = 6 \times 10^{-3}$  cm<sup>2</sup> V<sup>–1</sup> s<sup>–1</sup>;  $\mu_h = 4 \times 10^{-3}$  cm<sup>2</sup> V<sup>–1</sup> s<sup>–1</sup>). These ambipolar TOF mobilities are considerably higher than the respective values reported for P3HT ( $\mu_e = 1.5 \times 10^{-4}$  cm<sup>2</sup> V<sup>–1</sup> s<sup>–1</sup> and  $\mu_h = 3 \times 10^{-4}$  cm<sup>2</sup> V<sup>–1</sup> s<sup>–1</sup> at  $E > 10^5$  V cm<sup>–1</sup>).<sup>12</sup>

(12) Choulis, S. A.; Kim, Y.; Nelson, J.; Bradley, D. D. C.; Giles, M.; Shkunov, M.; McCulloch, I. *Appl. Phys. Lett.* **2004**, *85*, 3890.

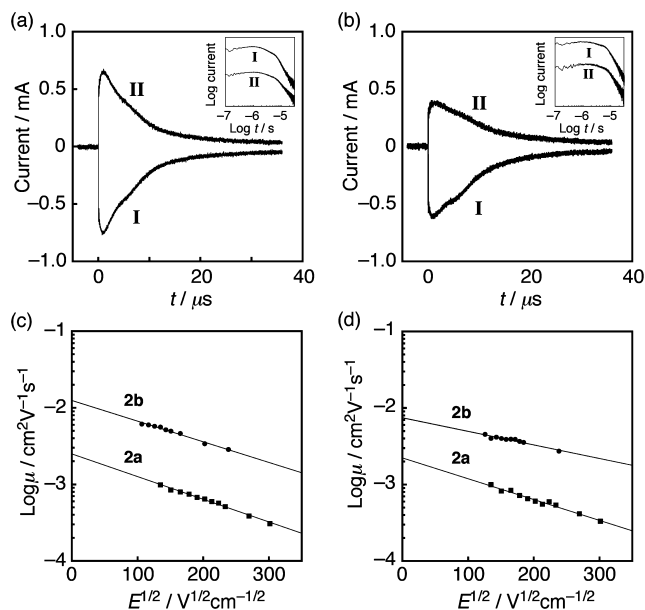


**Figure 4.** (a) TOF current transients observed for **2a** at electric field strengths ( $E$ ) of  $1.1 \times 10^4 \text{ V cm}^{-1}$  (I, positive bias mode) and  $1.6 \times 10^4 \text{ V cm}^{-1}$  (II, negative bias mode). (b) TOF current transients observed for **2b** at  $E = 1.8 \times 10^4 \text{ V cm}^{-1}$  (I, II). The log–log plots of TOF current transients vs time are also depicted as insets in (a) and (b). (c) Electron mobilities ( $\mu_e$ ) of **2a,b** vs  $E^{1/2}$ . (d) Hole mobilities ( $\mu_h$ ) of **2a,b** vs  $E^{1/2}$ .

To determine the effects of  $P$ -substituents on the short-range charge transport properties of polyphospholes, we next measured the charge carrier mobilities of **2a,b** by using a flash-photolysis time-resolved microwave conductivity (TRMC<sup>13</sup>) method (Table 1; Figure S6). This electrodeless method allows the conductivities of conjugated polymers to be investigated.<sup>14</sup> The flash photolysis of drop-cast films of **2a,b** with a 355-nm laser pulse promptly increased transient conductivity ( $\phi\Sigma\mu$ ), in which  $\phi$  is the quantum efficiency of charge separation and  $\Sigma\mu$  is the sum of mobilities of all the transient charge carriers, reaching the maximum transient conductivities of  $3.5 \times 10^{-5} \text{ cm}^2 \text{ V}^{-1} \text{ s}^{-1}$ . In the present study, the  $\phi$  values were independently determined from the transient absorption spectroscopy (TAS) of **2a,b**, where the upper limits of the amounts of charge carriers were estimated from differences in absorbance (bleaching due to consumption of the neutral species) at 620 nm. TAS allowed the lower limit of  $\Sigma\mu$  values to be determined. The  $\Sigma\mu$  values of **2a** and **2b** thus estimated

(13) For example, see: (a) Warman, J. M.; Gelinck, G. H.; de Haas, M. P. *J. Phys.: Condens. Mater.* **2002**, *14*, 9935. (b) Grozema, F. C.; Siebbeles, L. D. A.; Warman, J. M.; Seki, S.; Tagawa, S.; Scherf, U. *Adv. Mater.* **2002**, *14*, 228. (c) Saeki, A.; Koizumi, Y.; Aida, T.; Seki, S. *Acc. Chem. Res.* **2012**, *45*, 1193.

(14) For example, see: (a) Saeki, A.; Seki, S.; Koizumi, Y.; Sunagawa, T.; Ushida, K.; Tagawa, S. *J. Phys. Chem. B* **2005**, *109*, 10015. (b) Saeki, A.; Seki, S.; Sunagawa, T.; Ushida, K.; Tagawa, S. *Philos. Mag.* **2006**, *86*, 1261. (c) Saeki, A.; Seki, S.; Koizumi, Y.; Tagawa, S. *J. Photochem. Photobiol. A* **2007**, *186*, 158.

(15) Saeki, A.; Ohsaki, S.; Seki, S.; Tagawa, S. *J. Phys. Chem. C* **2008**, *112*, 16643.

**Table 1.** Charge Mobilities of Poly(phosphole  $P$ -imide)s **2a,b**

compd	TOF <sup>a</sup> $\mu_h/\text{cm}^2 \text{ V}^{-1} \text{ s}^{-1}$	TOF <sup>a</sup> $\mu_e/\text{cm}^2 \text{ V}^{-1} \text{ s}^{-1}$	TRMC <sup>b</sup> $\Sigma\mu/\text{cm}^2 \text{ V}^{-1} \text{ s}^{-1}$
<b>2a</b>	$1 \times 10^{-3}$ ( $2 \times 10^{-3}$ )	$1 \times 10^{-3}$ ( $2 \times 10^{-3}$ )	$>5 \times 10^{-3}$
<b>2b</b>	$4 \times 10^{-3}$ ( $7 \times 10^{-3}$ )	$6 \times 10^{-3}$ ( $1 \times 10^{-2}$ )	$>3 \times 10^{-2}$

<sup>a</sup> Hole/electron mobilities ( $\mu_h/\mu_e$ ) measured by the TOF method at  $E = 1.8 \times 10^4 \text{ V cm}^{-1}$ . The  $\mu_h/\mu_e$  values in parentheses are at  $E = 0 \text{ V cm}^{-1}$ , obtained by extrapolation from  $\log \mu - E^{1/2}$  plots. <sup>b</sup> Sum of charge carrier mobilities ( $\Sigma\mu$ ) measured by the TRMC method.

are  $>5 \times 10^{-3}$  and  $>3 \times 10^{-2} \text{ cm}^2 \text{ V}^{-1} \text{ s}^{-1}$ , respectively. Although the exact  $\mu_e$  and  $\mu_h$  values cannot be deduced from the present TRMC–TAS data, the charge carrier transport abilities of the poly(phosphole  $P$ -imide)s are comparable to those reported for P3HT ( $0.12 \text{ cm}^2 \text{ V}^{-1} \text{ s}^{-1}$  for regioregular P3HT and  $6 \times 10^{-3} \text{ cm}^2 \text{ V}^{-1} \text{ s}^{-1}$  for regiorandom P3HT, determined by the TRMC–TAS method),<sup>15</sup> representative of the fact that the phosphorus(V)-bridges provide highly conjugated polyacetylene  $\pi$ -networks for charge carriers.

In summary, we have established a divergent method for introducing solubilizing alkyl chains to the common phosphole synthons through  $P^V=N$  bond formation and successfully converted the monomers to the poly(phosphole  $P$ -imide)s. The new  $P^V$ -bridged  $\pi$ -conjugated polymers displayed extremely narrow HOMO–LUMO gaps due to the effectively conjugated  $\pi$ -networks. In addition, we have determined charge-carrier mobilities of the polyphospholes for the first time. It is noteworthy that poly(phosphole  $P$ -imide)s exhibited long-range charge-carrier mobilities of up to  $6 \times 10^{-3}/4 \times 10^{-3} \text{ cm}^2 \text{ V}^{-1} \text{ s}^{-1}$  (for electron/hole) by the TOF method. The present study exemplifies poly(phosphole  $P$ -imide)s as potential candidates for both n-type and p-type semiconducting materials. The small values of the long-range mobilities (TOF) compared to the short-range mobilities (TAS–TRMC) demonstrate how the intrachain  $\pi$ -networks intrinsically govern the bulk charge carrier transport property. In this context, the reduction of intermolecular segregation of the polymer chains of polyphospholes is the next subject of focus, and further studies on the synthesis of new phosphole-containing conjugated polymers are in progress.

**Acknowledgment.** This work was partially supported by a Grant-in-Aid (No. 22350016) from the MEXT, Japan. Y.M. deeply thanks Prof. Hideyuki Murata and Dr. Varun Vohra (JAIST) for their valuable comments on the electrochemical properties of polyphospholes.

**Supporting Information Available.** Experimental details, DFT calculation results, and CIF data. This material is available free of charge via the Internet at <http://pubs.acs.org>.

The authors declare no competing financial interest.